

Thermodynamically self-consistent theory of structure for three-dimensional lattice gases

Davide Pini and George Stell

Department of Chemistry, State University of New York at Stony Brook, Stony Brook, New York 11794-3400

Ronald Dickman

Department of Physics and Astronomy, Lehman College, City University of New York, Bronx, New York 10468-1589

(Received 15 September 1997)

Recently, methods were developed to solve with high accuracy the equations that describe a thermodynamically self-consistent theory for the two-body correlation function, and preliminary results were reported for three-dimensional lattice gases with nearest-neighbor attractive interaction [R. Dickman and G. Stell, Phys. Rev. Lett. **77**, 996 (1996)]. Here we give a detailed description of our methods and of the results, which are found to be remarkably accurate for both the thermodynamics and structure of these systems. In particular, critical temperatures are predicted to within 0.2% of the best estimates from series expansions. Although above the critical temperature the theory yields the same critical exponents as the spherical model, this asymptotic behavior sets in only in a very narrow region around the critical point, so that the apparent exponents and the thermodynamics are well reproduced up to reduced temperatures of around 10^{-2} . On the coexistence curve, on the other hand, the exponents are nonspherical, and considerably more accurate than the spherical ones. For instance, the exponent β_{coex} predicted by the theory for the shape of the coexistence curve is $\beta_{\text{coex}}=0.35$. [S1063-651X(98)01203-3]

PACS number(s): 05.50.+q, 05.70.Ce, 64.60.Cn, 64.60.Fr

I. INTRODUCTION

A widely adopted approach in the realm of liquid-state theory consists in closing the exact Ornstein-Zernike (OZ) equation linking the two-particle distribution function $g(r)$ and the direct correlation function $c(r)$ by some approximate relation expressing $c(r)$ in terms of the thermodynamic state of the system, the interparticle potential, and often $g(r)$ itself [1]. As is well known, these closure schemes generally lead to thermodynamic inconsistencies: for example, different pressures are obtained depending on whether one uses the virial, compressibility, or energy routes. Some years ago a remedy was proposed for this defect: while $c(r)$ is assumed to have always the same range as the potential—an ansatz of common use in the above mentioned methods, usually referred to as the OZ approximation—its dependence on the thermodynamic state is not given *a priori*. Rather, $c(r)$ is determined on the basis of consistency with a single-valued free energy function [2–4]. Despite the promise revealed in initial applications of this *self-consistent OZ approximation* (SCOZA), much remains to be explored regarding its accuracy for various fluid models. In this paper we apply the SCOZA to three-dimensional lattice gases with nearest-neighbor interactions. The present study extends and explicates the work reported in a recent Physical Review Letter [5] by presenting further results both in and away from the critical regime and by describing in some detail the theory and the numerical procedure. We have tested the quantitative accuracy of SCOZA predictions by comparing them with the results from approximants based on extrapolation of series expansions, which can be considered essentially exact for our purposes. We find that SCOZA describes quite accurately both the thermodynamics and the correlations over most of the phase diagram. In particular, the nonuniversal properties at the critical point, e.g., the critical temperature,

internal energy, etc., and the coexistence curve are very well reproduced. Above the critical temperature the theory exhibits the same critical exponents as the spherical model [6]. We find, however, that this asymptotic regime is very narrow, so that the observables and the *effective* exponents are in good agreement with the true behavior of the system until the temperature differs from its critical value by less than 1% or so. Moreover, the exponents along the coexistence curve are nonclassical, and considerably more accurate than the spherical ones: for instance, we find that the curvature of the coexistence curve is described by an exponent $\beta_{\text{coex}}=0.35$.

The plan of the paper is as follows. In Sec. II we describe the theory, which leads to a nonlinear partial differential equation for the inverse correlation length, and we cast this equation in a form suitable for numerical integration. The results of the numerical solution are described in Sec. III, where nonuniversal properties are considered, and in Sec. IV, where we focus instead on universal properties in the critical region. Our conclusions are provided in Sec. V. Some details about the algorithm adopted for the numerical solution of the equation are reported in an Appendix.

II. THEORY

We consider a three-dimensional lattice gas with nearest-neighbor attractive interaction. If \mathbf{r}_i and \mathbf{r}_j are the positions of two generic lattice sites i and j , the interparticle potential is

$$v(\mathbf{r}_i - \mathbf{r}_j) = \begin{cases} +\infty, & \mathbf{r}_i = \mathbf{r}_j \\ -w, & i, j \text{ nearest neighbors} \\ 0 & \text{otherwise,} \end{cases} \quad (1)$$

where w is the strength of the nearest-neighbor potential ($w > 0$). For this system the above mentioned OZ approxi-

mation introduces a key simplification, since assuming that the direct correlation function $c(\mathbf{r})$ has the same range as the potential implies that $c(\mathbf{r})$ is truncated at nearest-neighbor separation. This gives only two nonvanishing values for $c(\mathbf{r})$, namely, the on-site one c_0 and the nearest-neighbor one c_1 . A relation between c_0 and c_1 is provided by the *core condition*, i.e., the (exact) requirement that the radial distribution function $g(\mathbf{r}_i - \mathbf{r}_j)$ must vanish for $i=j$ due to the singular on-site repulsion in the potential (1), which forbids multiple occupancy of each lattice site. As is well known [7,8], for a nearest-neighbor lattice gas the OZ approximation and the core condition enable one to express both the thermodynamics and the correlations as a function of a single state-dependent quantity. To this end, let us introduce the total correlation function $h(\mathbf{r}) = g(\mathbf{r}) - 1$. This is related to the direct correlation function by the OZ equation, which for a lattice system reads

$$h(\mathbf{r}_i) = c(\mathbf{r}_i) + \rho \sum_j c(\mathbf{r}_j) h(\mathbf{r}_i - \mathbf{r}_j), \quad (2)$$

where the number density ρ is the average number of particles per lattice site, and the sum is over all the lattice sites. In Fourier space, Eq. (2) yields

$$1 + \rho \tilde{h}(\mathbf{k}) = \frac{1}{1 - \rho \tilde{c}(\mathbf{k})}, \quad (3)$$

where $\tilde{c}(\mathbf{k})$ is given by

$$\tilde{c}(\mathbf{k}) = c_0 + \frac{q}{r} c_1 \Phi(\mathbf{k}). \quad (4)$$

Here q is the number of nearest neighbors, while $r=3$ for the simple cubic (sc) and the face centered cubic (fcc) lattice, and $r=1$ for the body centered cubic (bcc) lattice (r is the number of subgroups invariant under inversions). The nearest-neighbor sum $\Phi(\mathbf{k})$ is

$$\Phi(k) = \begin{cases} \cos k_x + \cos k_y + \cos k_z, & \text{sc} \\ \cos k_x \cos k_y \cos k_z, & \text{bcc} \\ \cos k_x \cos k_y + \cos k_x \cos k_z + \cos k_y \cos k_z, & \text{fcc} \end{cases} \quad (5)$$

where it is understood that lengths are measured in units of the (nonvanishing) components of the nearest-neighbor lattice vectors. By use of Eq. (3) the core condition $h(r=0) = -1$ becomes

$$\int \frac{d^3 \mathbf{k}}{(2\pi)^3} \frac{1}{1 - \rho \tilde{c}(\mathbf{k})} = 1 - \rho. \quad (6)$$

If we introduce the variable

$$z = \frac{q\rho c_1}{1 - \rho c_0} \quad (7)$$

and the function

$$P(z) = \int_0^\pi \frac{d^3 \mathbf{k}}{\pi^3} \frac{1}{1 - (z/r)\Phi(\mathbf{k})} \quad (8)$$

Eq. (6) gives then

$$c_0 = \frac{1}{\rho} \left[1 - \frac{P(z)}{1 - \rho} \right], \quad (9)$$

$$c_1 = \frac{zP(z)}{q\rho(1 - \rho)}. \quad (10)$$

The function $P(z)$ introduced in Eq. (8) is the Green function for the Helmholtz equation on a lattice. This function has been studied by a number of authors [9–12], and can be evaluated in terms of elliptic integrals. For instance, for the bcc lattice one has [10]

$$P(z) = \frac{4}{\pi^2} [K(s)]^2, \quad (11)$$

where $K(s)$ is the complete elliptic integral of the first kind,

$$K(s) = \int_0^{\pi/2} \frac{d\theta}{\sqrt{1 - s^2 \sin^2 \theta}} \quad (12)$$

and

$$s^2 = \frac{1}{2} [1 - \sqrt{1 - z^2}]. \quad (13)$$

Similar, but more complex expressions are known for the other lattices [11,12]. It is easily seen that the variable z is related to the correlation length ξ defined by $1/S(k) \sim \chi_{\text{red}}^{-1}(1 + \xi^2 k^2)$, $k \rightarrow 0$, where $S(\mathbf{k}) = 1/[1 - \rho \tilde{c}(\mathbf{k})]$ is the structure factor. Specifically, one has $\xi^2/l^2 = z/[q(1 - z)]$, l being the size of the unit cell. The value of the total correlation function at nearest-neighbor separation h_1 is readily obtained by setting $\mathbf{r}_i = \mathbf{0}$ in the OZ equation (2). One then gets

$$h_1 = -\frac{1}{q\rho c_1} [1 + (1 - \rho)c_0] = -\frac{1 - \rho}{\rho} \frac{1 - P(z)}{zP(z)}, \quad (14)$$

where Eqs. (9) and (10) have been used.

As stated in the Introduction, most OZ theories are characterized by an explicit closure relation in which the direct correlation function is related to the microscopic interaction, and typically to the total correlation function h as well. For the nearest-neighbor lattice gas this gives a relation for c_1 which, combined with Eq. (10), yields a closed equation for z [7,8]. In SCOZA, by contrast, c_1 is implicitly determined by requiring that the compressibility and internal energy routes to the thermodynamics lead to the same results. This requirement is embodied in the relation

$$\frac{\partial}{\partial \beta} \left(\frac{1}{\chi_{\text{red}}} \right) = \rho \frac{\partial^2}{\partial \rho^2} (\rho u), \quad (15)$$

where χ_{red} is the reduced isothermal compressibility as obtained from the structure factor at zero wave vector, u is the

internal energy per particle as obtained by the so-called internal-energy rule [1], and $\beta = 1/(k_B T)$, T being the absolute temperature, and k_B the Boltzmann constant. In the following, energies and temperatures will be measured in units of w and w/k_B , respectively. From Eqs. (9), (10), and (14) we get

$$\frac{1}{\chi_{\text{red}}} = 1 - \rho(c_0 + qc_1) = \frac{(1-z)P(z)}{1-\rho}, \quad (16)$$

$$u = -\frac{1}{2}q\rho(1+h_1) = -\frac{1}{2}q\rho + \frac{1}{2}q(1-\rho)\frac{1-P(z)}{zP(z)}. \quad (17)$$

From Eqs. (10) and (16) it can be seen that in the physically meaningful region one has $0 \leq z \leq 1$. In particular, $z=0$ corresponds to the low-density or high-temperature limit, while $z=1$ gives the locus of diverging compressibility, so that $z=1$ at the critical point. Since the lattice Green function diverges at $z=1$ for lattice dimensionality $d \leq 2$, SCOZA and more generally any OZ theory incorporating the core condition predicts that the critical temperature T_c will vanish in one and two dimensions. We expect a finite value of T_c in two dimensions only if $c(\mathbf{r})$ is allowed to develop a power-law tail at the critical point.

By inserting Eqs. (16) and (17) into Eq. (15) the following partial differential equation (PDE) in the unknown function $\varphi(\rho, \beta)$ is obtained:

$$\frac{1}{\rho(1-\rho)} \frac{\partial}{\partial \beta} [(1-z)P(z)] = -\frac{q}{2} \frac{\partial^2}{\partial \rho^2} \left[\rho(1-\rho) \frac{P(z)-1}{zP(z)} \right] - q. \quad (18)$$

Equation (18) can be rewritten as a nonlinear diffusion equation. To this end, let us introduce the new unknown function

$$\varphi = \rho(1-\rho) \frac{P(z)-1}{zP(z)}, \quad (19)$$

which is proportional to the contribution to the internal energy per unit volume due to the fluctuations. In the physical non-negative compressibility region the function $y = [P(z) - 1]/[zP(z)]$ can be inverted to express z as $z = F(y)$. It is then readily found that Eq. (18) becomes

$$\frac{(1-y)F'(y) - F(y)[1-F(y)]}{[1-yF(y)]^2} \frac{\partial \varphi}{\partial \beta} = q[\rho(1-\rho)]^2 \left[\frac{1}{2} \frac{\partial^2 \varphi}{\partial \rho^2} + 1 \right], \quad (20)$$

where we have set $y = \varphi/[\rho(1-\rho)]$. The advantage of this diffusivelike form with respect to the original Eq. (18) lies in the fact that the numerical integration of Eq. (20) is much less cumbersome, and can be easily carried out without generating any instability in the critical or subcritical region. The finite-difference scheme employed by us is a predictor-corrector implicit algorithm expressly devised for this kind of *quasilinear* diffusion PDE [13]. Further details about the numerical algorithm are reported in the Appendix. While the

present method is preferable to that used in Ref. [5], we obtained fully consistent results using the two integration schemes. To integrate Eq. (20), the initial condition at $\beta = 0$ and two boundary conditions at low and high density are also needed. Since z vanishes both for $\beta=0$ and for $\rho=0$ and for small z one has $P(z) \sim 1 + z^2/q$, Eq. (19) yields

$$\varphi(\rho, \beta=0) = 0 \text{ for every } \rho, \quad (21)$$

$$\varphi(\rho=0, \beta) = 0 \text{ for every } \beta. \quad (22)$$

Moreover, since Eqs. (18) and (20) preserve particle-hole symmetry, the integration of Eq. (20) can be restricted in the interval $0 \leq \rho \leq 1/2$ by imposing the further boundary condition

$$\varphi\left(\frac{1}{2} + \Delta\rho, \beta\right) = \varphi\left(\frac{1}{2} - \Delta\rho, \beta\right), \quad (23)$$

where $\Delta\rho$ is the distance between two neighboring points of the density grid. Below the critical temperature the condition $0 \leq z \leq 1$ is fulfilled only outside a certain interval $(\rho_s, 1 - \rho_s)$, where $\rho_s = \rho_s(\beta)$ gives the locus of diverging compressibility for which $z=1$, i.e., the spinodal curve predicted by the theory. In the numerical integration of Eq. (20) we have excluded the thermodynamically unstable region bounded by the spinodal curve. Whenever for a certain density ρ_0 the quantity $\varphi(\rho_0, \beta)$ exceeds the value $\rho_0(1-\rho_0)[P(1)-1]/P(1)$, which corresponds to $z=1$, the integration is restricted to the density interval $(0, \rho_0 - \Delta\rho)$. Within the accuracy of the numerical mesh, $\rho_0 - \Delta\rho$ can be identified with the density ρ_s on the spinodal. For subcritical temperatures the high-density boundary condition (23) is therefore replaced by

$$\varphi(\rho_s, \beta) = \rho_s(1-\rho_s) \frac{P(1)-1}{P(1)}. \quad (24)$$

Once the quantity φ has been determined, z is obtained as $z = F[\varphi/\rho(1-\rho)]$. Equations (16) and (17) then yield the reduced compressibility χ_{red} and the internal energy per particle u . The pressure p and the chemical potential μ can be obtained by integrating, respectively, $1/\chi_{\text{red}}$ and $1/(\rho\chi_{\text{red}})$ with respect to the density. In the subcritical region the low- and high-density branches of the isotherms are separated by the spinodal, so that on the high-density branch such a procedure requires the pressure at a given point. This can be obtained by expanding $1/\chi_{\text{red}}$ in powers of ρ at low density and by exploiting the symmetry of $1/(\rho\chi_{\text{red}})$ around $\rho=1/2$. Integration with respect to $1-\rho$ then yields a high-density expansion for p , that can be used to determine p at the next-to-largest density $1-\Delta\rho$. For instance, for the sc lattice and $\rho \rightarrow 1$ one has

$$\beta p \sim -\ln(1-\rho) - 3\beta + 6f(1-\rho) - 3f(1+3f)(1-\rho)^2, \quad (25)$$

where $f \equiv e^\beta - 1$. Alternatively, one may differentiate the internal energy per particle with respect to ρ , and then integrate with respect to β to get the pressure and the chemical potential via the relations $\partial(\beta p)/\partial\beta = \rho^2 \partial u/\partial\rho$, $\partial(\beta\mu)/\partial\beta = u + \rho \partial u/\partial\rho$. Thanks to the thermodynamic consistency

TABLE I. Critical parameters of the nearest-neighbor lattice gas. The SCOZA results for the inverse critical temperature β_c , the internal energy per particle u_c , the entropy per particle s_c , and the pressure p_c are compared with the best-estimate results (indicated with the subscript ‘‘BE’’) obtained from extrapolation of series expansions for the sc, the bcc, and the fcc lattices. Energies and temperatures are in units of the interaction strength w and of w/k_B , respectively.

Lattice	$\beta_{c,\text{SCOZA}}$	$\beta_{c,\text{BE}}$	$u_{c,\text{SCOZA}}$	$u_{c,\text{BE}}$	$s_{c,\text{SCOZA}}$	$s_{c,\text{BE}}$	$(\beta p)_{c,\text{SCOZA}}$	$(\beta p)_{c,\text{BE}}$
sc	0.88503	0.88662 ^a	-2.0108	-1.9961 ^b	1.1035	1.1158 ^b	0.1140	0.1124
bcc	0.62852	0.62947 ^c	-2.5645	-2.5464 ^b	1.1532	1.1641 ^b	0.1255	0.1244
fcc	0.40775	0.40825 ^c	-3.7690	-3.7423 ^b	1.1700	1.1804 ^b	0.1301	0.1292

^aReference [14].

^bReference [19].

^cReference [15].

enforced by Eq. (20), this is equivalent to integration with respect to ρ , and furthermore it does not require prior knowledge of the high-density behavior. As a test of our numerical solution, we have checked that these two paths actually lead to the same thermodynamics. Once the pressure on the low- and high-density branches of the subcritical isotherms is known, the coexistence curve can be determined by means of a Maxwell construction. For the lattice gas this is simple, since particle-hole symmetry implies that the two branches of the coexistence curve in the density-temperature plane $\rho_v(\beta)$ and $\rho_l(\beta)$ are symmetric about $\rho=1/2$. Finding the coexisting densities therefore reduces to finding the density ρ_v such that $p(\rho_v, \beta) = p(1 - \rho_v, \beta)$.

III. RESULTS

In the present section we concentrate on SCOZA predictions for nonuniversal properties. Universal features of the critical behavior of the theory will be discussed in the next section.

The critical point predicted by Eq. (20) is determined by locating the divergence of the isothermal compressibility on the critical isochore. Since this equation preserves particle-hole symmetry, SCOZA correctly yields the value $\rho_c=1/2$ for the critical density of the lattice gas. The inverse critical temperature β_c is then obtained as the value of β for which $1/\chi_{\text{red}}$ vanishes. The algorithm employed for the numerical solution of Eq. (20) allows one to determine β_c up to a prescribed accuracy. The results, listed in Table I, are within 0.2% of the best series estimates [14,15] (in each case SCOZA underestimates β_c). For comparison, we note that for the sc lattice simple mean-field theory yields $\beta_c=2/3$, the quasichemical approximation yields $\beta_c=0.811$, and the Kikuchi approximation with a square and a cubic cluster yield, respectively, $\beta_c=0.868$ and $\beta_c=0.874$ [16]. The SCOZA value of the critical temperature is even more accurate than that predicted by two sophisticated closed-form approximations, the variational scheme devised by Baxter and Forrester [17] and the renormalization-group based hierarchical reference theory (HRT) [18]. For the sc lattice the former of these theories yields again $\beta_c=0.874$, and in general for the lattices considered here the error is in the 1–3 % range, despite the fact that it exactly reproduces many terms (up to 23, for the bcc lattice) in the low-temperature expansion for the free energy. HRT predicts instead $\beta_c=0.883$. Table I also includes data on the critical values of the entropy per

particle s_c , the internal energy per particle u_c , and the pressure p_c . We note that in the SCOZA, u_c can be determined directly from Eq. (17) as $u_c = -q [2P(1) - 1]/[4P(1)]$. While the mean spherical approximation gives the same u_c as the SCOZA, it predicts $\beta_c = 4P(1)/q$, which, as is well known, considerably overestimates β_c (by as much as 14% for the sc lattice). The difference between the SCOZA results and the best estimates from series analysis [19], also reported in Table I, is at most 0.7% for the critical internal energy, 1.1% for the critical entropy, and about 1.4% for the critical pressure. In Fig. 1 the reduced isothermal compressibility and the correlation length of the sc lattice on the critical isochore ($T > T_c$) and on the coexistence curve ($T < T_c$) are compared with Padé

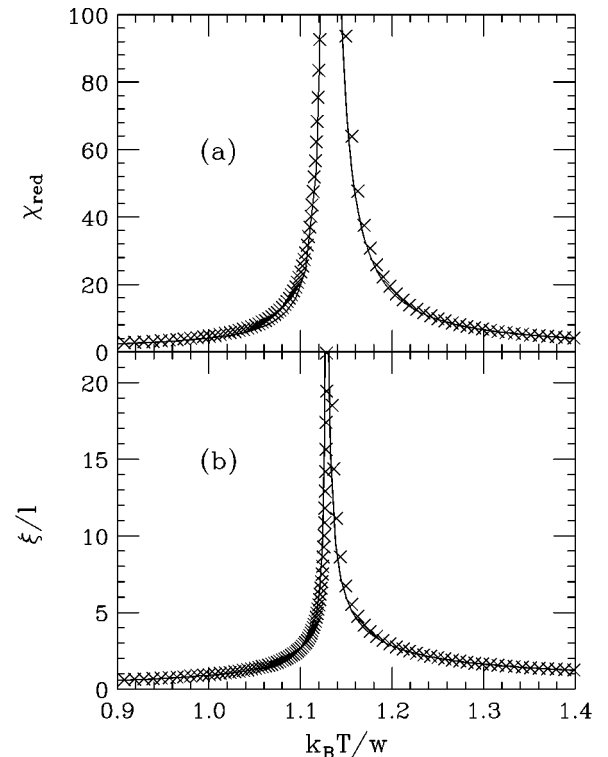


FIG. 1. Reduced isothermal compressibility χ_{red} (a) and correlation length ξ (b) of the sc lattice gas on the critical isochore ($T > T_c$) and on the low-density branch of the coexistence curve ($T < T_c$) as a function of the dimensionless temperature $k_B T/w$. ξ is in units of the lattice spacing l . Crosses: SCOZA. Solid line: approximant [20,21].

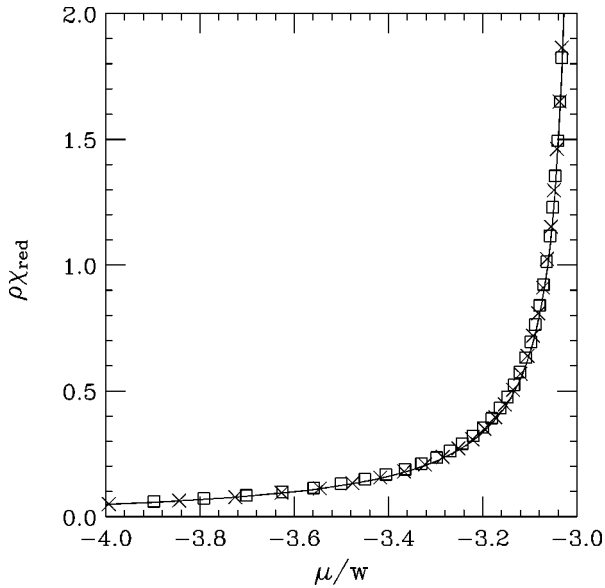


FIG. 2. Reduced isothermal compressibility on the critical isotherm of the sc lattice gas. The quantity $\rho\chi_{\text{red}}$ is plotted as a function of the chemical potential μ (in units of the interaction constant w). Crosses: SCOZA. Squares: HRT [18]. Solid line: approximant [21].

approximants to high- and low-temperature series [20,21]. The close agreement between SCOZA predictions and series estimates persists quite near the critical point. The compressibility on the critical isotherm of the sc lattice is shown in Fig. 2, where again an approximant [21] and the HRT result [18] are reported for comparison. It is worthwhile observing that in the present application of SCOZA both the second and the third virial coefficient are correctly reproduced [this property has been used to determine the expansion (25)], although this feature is not intrinsic to SCOZA, but it depends on the quite special character of a nearest-neighbor potential. In Fig. 3 we plot the specific heat at constant volume c_V of the bcc lattice on the critical isochore. As will be seen in the next section, this quantity does not diverge in SCOZA as $T \rightarrow T_c$. Nevertheless, the SCOZA result is in close agreement with the series predictions [22] over a wide range of temperatures. The coexistence curve of the sc lattice in the temperature-density plane is shown in Fig. 4 together with a Padé approximant from the low-temperature magnetization series [23]; we also show the predictions of the Kikuchi [24] theory on a square cluster and of the HRT [18]. Evidently, the SCOZA provides quite an accurate coexistence curve: it appears then that this theory continues to be reliable in the low-temperature regime. Finally, in Fig. 5 we show the structure factor of the sc lattice for $\rho = 1/2$ and two different temperatures along the direction $k_x = k_y = k_z$ of the Brillouin zone. Also shown are a closed-form approximant [20] and the results from the mean spherical approximation (MSA) [7,8] and from the HRT [18]. Unlike the MSA, both the HRT and the SCOZA are in very satisfactory agreement with the approximant, with the SCOZA performing slightly better at small k .

IV. CRITICAL BEHAVIOR

In Fig. 6 the isothermal compressibility of the sc lattice on the critical isochore is plotted as a function of the reduced

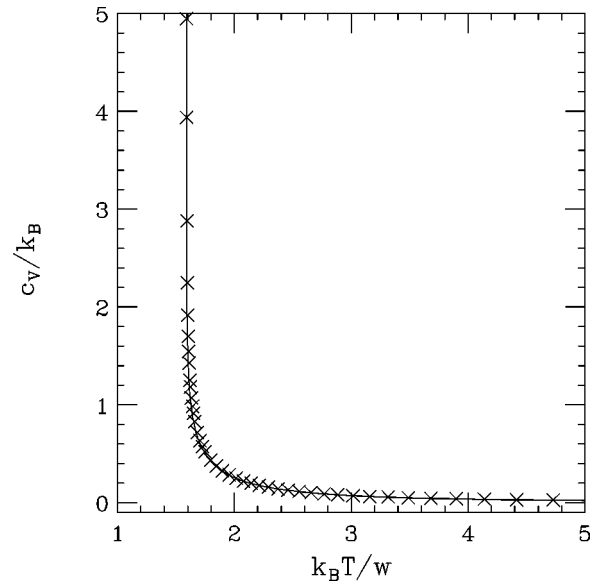


FIG. 3. Specific heat (thermal capacity per particle) at constant volume c_V on the critical isochore of the bcc lattice gas as a function of the dimensionless temperature $k_B T/w$. Crosses: SCOZA. Solid line: approximant [22].

temperature $t = (T - T_c)/T_c$ on a log-log scale (for each of the approximations shown in the figure, the correspondent value of T_c has been used to determine t). It appears that in SCOZA the divergence of the compressibility as T_c is approached is asymptotically governed by a power law with a critical exponent $\gamma = 2$: this coincides with the value of γ predicted by MSA [7,8], whose exponents in turn are those of the spherical model. Indeed, our results show that above the critical temperature T_c the asymptotic critical behavior of SCOZA is the same as in MSA: besides $\gamma = 2$, we have then $\delta = 5$ and $\alpha = -1$, where we have adopted the standard notation for the critical exponents. Those values are of course

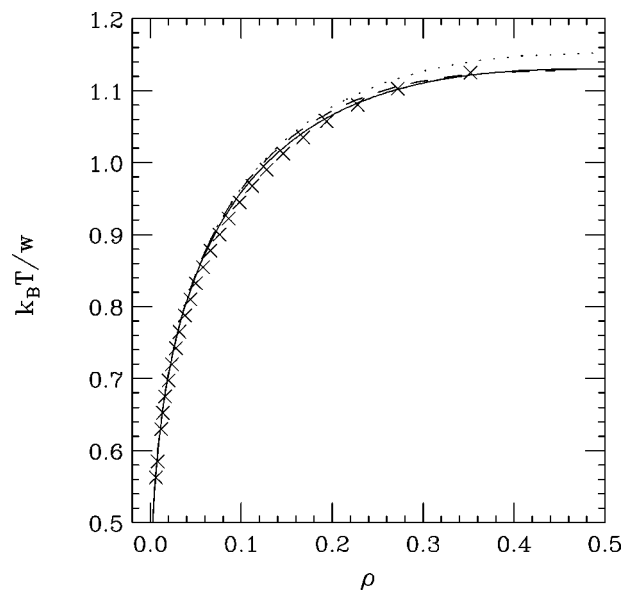


FIG. 4. Coexistence curve of the sc lattice gas in the temperature-density plane. Solid line: SCOZA. Crosses: HRT [18]. Dotted line: Kikuchi theory with a square cluster [24]. Dashed line: approximant [23].

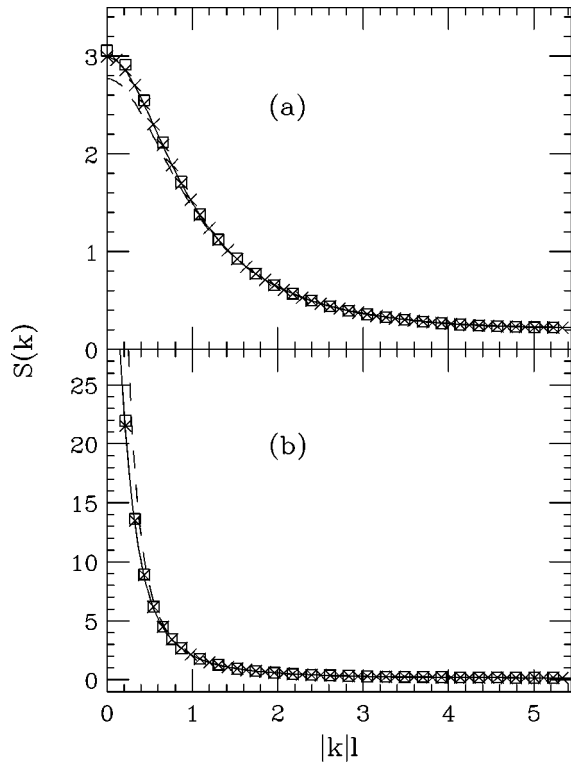


FIG. 5. Structure factor $S(\mathbf{k})$ of the sc lattice gas along the direction $k_x = k_y = k_z$ of the Brillouin zone as a function of the norm of \mathbf{k} (in units of the reciprocal of the lattice spacing l) at $\rho = 1/2$. The predictions from different theories and from the approximant are compared at the same temperature $k_B T/w = 1.5$, for which the ‘‘exact’’ reduced temperature is $T/T_c \approx 1.33$ (a), and at reduced temperature $T/T_c = 1.03$ (b). Crosses: SCOZA. Squares: HRT [18]. Dashed line: MSA. Solid line: approximant [20].

quite inaccurate, the true ones being [25] $\gamma \approx 1.24$, $\delta \approx 4.8$, $\alpha \approx 0.1$. However, the onset of the asymptotic critical regime appears to be very different than in MSA: this can be better appreciated by introducing an *effective exponent* defined as the local slope of the log-log plot of the quantity of interest. The effective exponents γ_{eff} and δ_{eff} are plotted in Figs. 6 and 7, respectively. It can be seen that the ‘‘exact’’ γ_{eff} (that is, the one predicted by the approximant [21]) reaches its asymptotic value for $t \sim 10^{-2}$. This is true also for MSA and for HRT [18], whose predictions are also shown in Fig. 6 (HRT yields the nonclassical value $\gamma \approx 1.378$ [26]). SCOZA, by contrast, is affected by a strong crossover from a nearly exact to a MSA-like behavior, so that $\gamma = 2$ is obtained only for $t \sim 10^{-5}$. Therefore the MSA critical indices affect SCOZA thermodynamics only in a narrow neighborhood of the critical point. For instance, for $t > 0.015$ the relative error in the isothermal compressibility is less than 10%, and for $t > 0.1$ it is less than 0.5%. The specific heat at constant volume of the sc lattice on the critical isochore for $t \rightarrow 0$ is shown in Fig. 8, together with the approximant [22] and the HRT [27] results. Although in the SCOZA (as well as in the HRT) this quantity does not diverge at the critical point, the saturation does not become evident until $t \sim 10^{-4}$.

It is worthwhile noting that the evidence of spherical critical exponent for $T > T_c$ does not agree with the conclusions of a previous analysis [4,8] based on the form assumed by Eq. (18) close to the critical point, i.e., for $z \rightarrow 1$, according

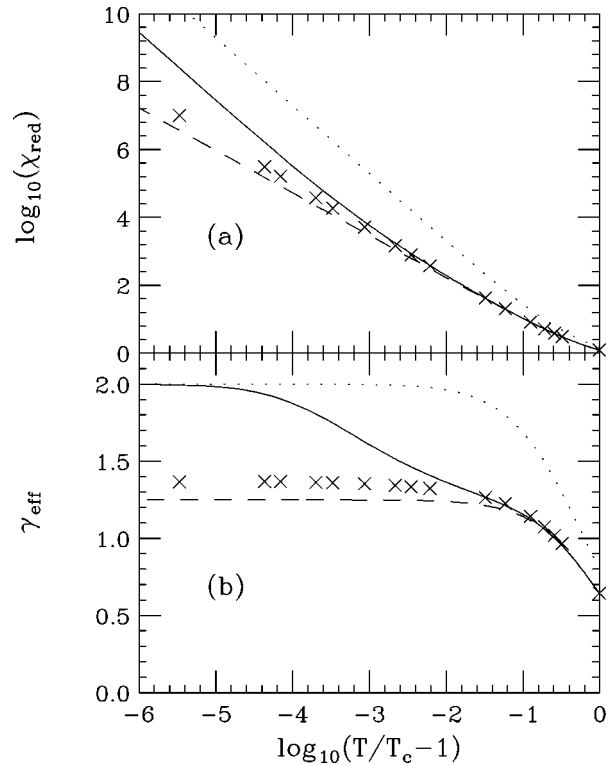


FIG. 6. Log-log plot of the reduced isothermal compressibility χ_{red} on the critical isochore (sc lattice) as a function of the reduced temperature $(T - T_c)/T_c$ (a) and corresponding effective exponent γ_{eff} (b). Solid line: SCOZA. Crosses: HRT [18]. Dotted line: MSA. Dashed line: approximant [21].

to which SCOZA would exhibit a scaling equation of state with the Gaussian three-dimensional exponents $\gamma = 1$, $\delta = 5$, $\alpha = 1/2$. Further investigation shows that this is not the only possible scaling solution, and that in the critical region Eq. (18) does have a solution that behaves as

$$z \sim 1 - [a(\rho - \rho_c)^2 + bt]^2, \quad (26)$$

where a and b are constants. By using the expansion of the lattice Green functions for $z \rightarrow 1$ [10–12],

$$P(z) \sim P(1) - d\sqrt{1-z} + O(1-z), \quad (27)$$

it is readily seen from Eq. (16) that Eq. (26) gives rise to MSA-like scaling in the equation of state, in agreement with our numerical results. Thus we conclude that above T_c the critical behavior of SCOZA is described by Eq. (26). In particular, the amplitude a of the $(\rho - \rho_c)^2$ term is related to the coefficients of the expansion (27) by $a = 4P(1)/d$. If Eqs. (26) and (27) are substituted into the expression (10) for the direct correlation function at nearest-neighbor separation c_1 , an expansion for c_1 around its critical value $c_{1,c}$ in powers of $(\rho - \rho_c)^2$ and t is obtained:

$$c_1 \sim c_{1,c} + A_4 (\rho - \rho_c)^4 + B_1 t + \dots, \quad (28)$$

where the coefficient A_2 of $(\rho - \rho_c)^2$ vanishes due to the particular value of a . Such behavior, which has been checked numerically, is consistent with a previous result [7] according to which, whenever c_1 is analytic in $(\rho - \rho_c)^2$ and t ,

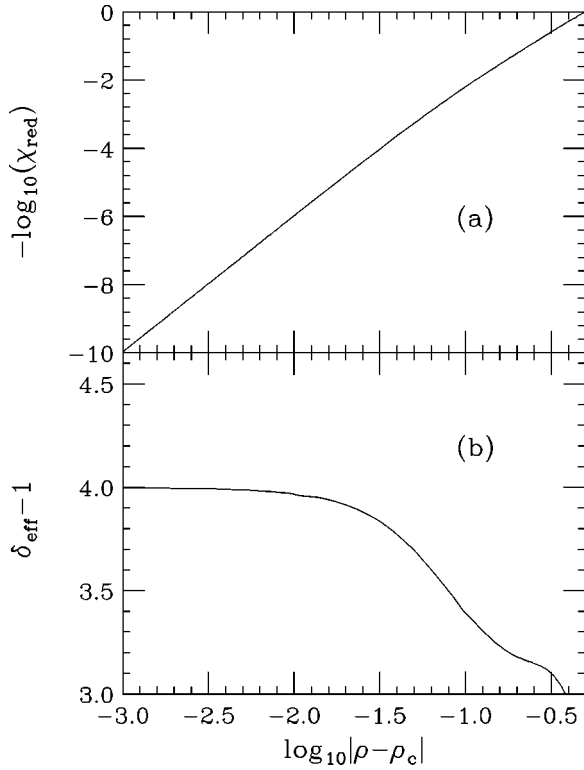


FIG. 7. Log-log plot of the reciprocal of the reduced isothermal compressibility χ_{red} on the critical isotherm of the bcc lattice (low-density branch) as a function of the reduced density $|\rho - \rho_c|$ (a) and corresponding effective exponent $\delta_{\text{eff}} - 1$ (b) according to SCOZA.

spherical-model exponents are obtained provided one has $A_2 < c_{1,c}/\rho_c^2$. This condition is manifestly satisfied in the present case, in which $A_2 = 0$.

Quite surprisingly, below T_c the critical behavior of SCOZA does not coincide with the one just described. In

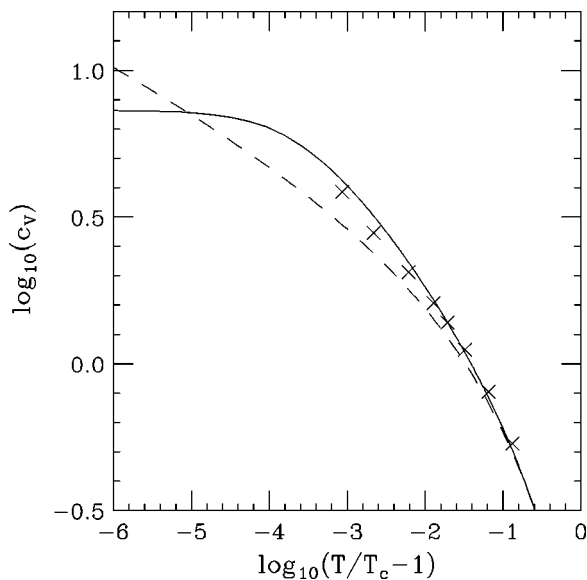


FIG. 8. Log-log plot of the specific heat at constant volume c_V on the critical isochore (sc lattice) as a function of the reduced temperature $(T - T_c)/T_c$. Solid line: SCOZA. Crosses: HRT [18]. Dashed line: approximant [22]. Both SCOZA and HRT predict a finite value for the specific heat at the critical point.

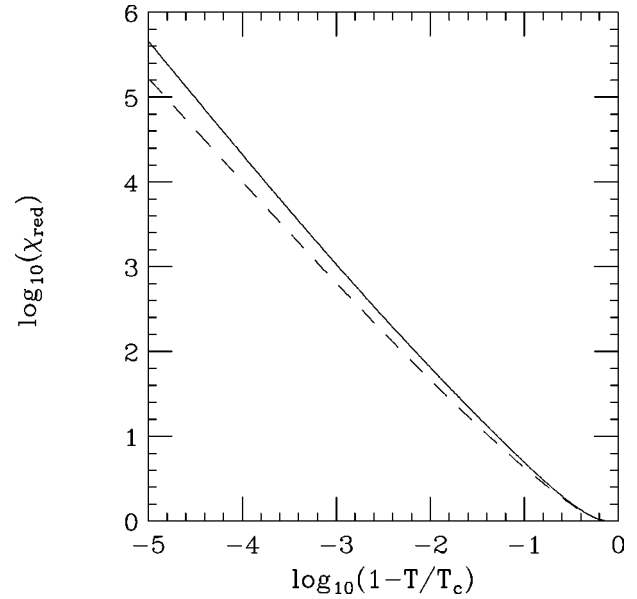


FIG. 9. Log-log plot of the reduced isothermal compressibility χ_{red} on the low-density branch of the coexistence curve as a function of the reduced temperature $(T_c - T)/T_c$ (bcc lattice). Solid line: SCOZA. Dashed line: approximant [15].

fact, while MSA scaling predicts that along the spinodal curve $\rho - \rho_c$ will vanish for $t \rightarrow 0$ as $|\rho - \rho_c| \sim |t|^{\beta_{\text{spin}}}$ with $\beta_{\text{spin}} = 1/2$, we find instead that SCOZA has $\beta_{\text{spin}} = 3/4$. Moreover, for a lattice gas in three dimensions the MSA fails to give a coexistence curve close to the critical point on the basis of Eq. (16) [7], which is not the case with SCOZA. Instead, it is found both analytically and numerically that along the SCOZA coexistence curve χ_{red} , $|\rho - \rho_c|$, and c_V assume a power-law behavior with effective critical exponents that take on the limiting values at critical of $\gamma' = 7/5$, $\beta_{\text{coex}} = 7/20$, $\alpha' = -1/10$. These are considerably more accurate than either the MSA or the mean-field values, especially in the case of β_{coex} . Log-log plots of the isothermal compressibility and of the reduced density together with its effective exponent $\beta_{\text{coex}}^{\text{eff}}$ are shown in Figs. 9 and 10, respectively, where the results from the approximants [15] are also shown (the “exact” value of the exponent β_{coex} is $\beta_{\text{coex}} \approx 0.33$). We note again that the asymptotic regime is reached only in a very narrow neighborhood of the critical point ($|t| \approx 10^{-5} - 10^{-6}$). The difference between the exponents on the critical isochore for $T > T_c$ and the corresponding ones on the coexistence curve for $T < T_c$ is a feature of the SCOZA that is presumably an artifact of the approximation; it is not expected to be a feature of the exact behavior of the model. It stems from an extended form of scaling behavior that characterizes the SCOZA thermodynamics close to the critical point. In contrast, the exact lattice-gas behavior is widely believed to be given by a simpler form of thermodynamic scaling in which exponents below and above the critical temperature are identical.

It is worthwhile stressing that the extended scaling does not imply any spurious singularity in the equation of state when the $T = T_c$ axis is crossed at noncritical density. In fact, the same critical isotherm and the exponent $\delta = 5$ are recovered both from above and from below T_c . Moreover, the standard algebraic relations among the critical exponents are

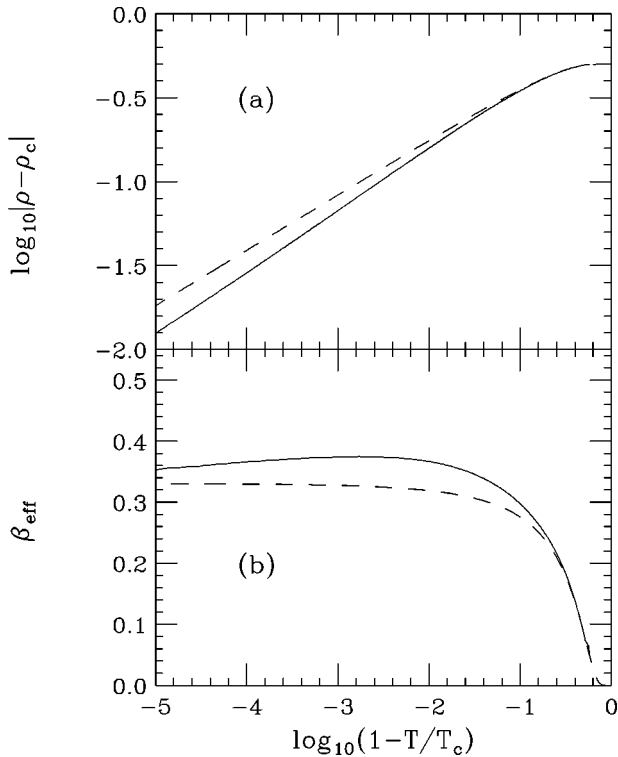


FIG. 10. Log-log plot of the reduced density $|\rho - \rho_c|$ on the coexistence curve (bcc lattice) as a function of the reduced temperature $(T_c - T)/T_c$ (a) and corresponding effective exponent $\beta_{\text{coex}}^{\text{eff}}$ (b). Solid line: SCOZA. Dashed line: approximant [15].

satisfied in both cases. The z that is associated with the extended scaling is given by

$$z \sim 1 - \left[a(\rho - \rho_c)^2 + bt\psi_{\pm} \left(\frac{|\rho - \rho_c|}{|t|^{1/4}} \right) \right]^2, \quad (29)$$

where the functions ψ_+ , ψ_- account for the different behavior, respectively, above and below T_c : in particular, as is readily seen from Eq. (26), one has simply $\psi_+ \equiv 1$, while ψ_- is not constant and goes to 1 only when its argument diverges. This form of z was revealed in an investigation by two of us in collaboration with Høye that we plan to report on in a separate paper containing derivations as well as analytic and numerical details [28]. Some time ago it was pointed out by one of us [29] that the very fact that scaling can only be expected in an approximate sense (i.e., locally, about the critical point) gives rise to the possibility of a mechanism yielding $\gamma \neq \gamma'$, $\nu \neq \nu'$, etc. Such an asymmetry was subsequently found to characterize the exact behavior of certain rather special models [30]. It is interesting to find that the imposition of self-consistency along with the core condition and an Ornstein-Zernike ansatz on the form of $c(\mathbf{r})$ is in fact enough to trigger just such a mechanism, although *not* the precise form of the scaled thermodynamics discussed in [29] or found in [30].

V. CONCLUSIONS

We have applied a thermodynamically self-consistent OZ approximation, along the lines proposed by Høye and Stell [2–4], to nearest-neighbor attractive lattice gases in three

dimensions. The accuracy of the results is remarkable: the critical temperatures are reproduced with an error of less than 0.2%, and outside the immediate vicinity of the critical point the error on the coexistence curves does not exceed 2%. Above the critical temperature SCOZA predicts the same critical exponents as the mean spherical approximation, but this asymptotic behavior is detectable only in a very narrow neighborhood of the critical point. Therefore the thermodynamics remains accurate up to reduced temperatures around 10^{-2} . As a result of an extended form of scaling behavior shown by SCOZA, the exponents on the coexistence curve do not coincide with the spherical values. These exponents turn out to be both nonspherical and nonclassical, and are considerably more accurate than either the spherical or the mean-field ones.

Our results suggest that the application of SCOZA to other three-dimensional systems will prove most useful. A further interesting feature of the theory in this respect is that a single run of integration sweeps the whole density-temperature plane, so that the thermodynamics and the phase diagram are obtained at once. The study of a fluid of spherical particles with a repulsive core and a Yukawa attractive tail potential is currently under way [31]. We are also investigating improving the approximation by extending the range of $c(\mathbf{r})$.

ACKNOWLEDGMENTS

We are grateful to Johan Høye for many helpful discussions and correspondence and to Alberto Parola for sending us his HRT results for the specific heat. G.S. is indebted to the National Science Foundation for support of this work while D.P. and R.D. gratefully acknowledge the support of the Division of Chemical Sciences, Office of Basic Energy Sciences, Office of Energy Research, U.S. Department of Energy.

APPENDIX

In this appendix some details about the algorithm adopted for the numerical integration of the PDE (20) are provided. This is a nonlinear diffusion equation of the form

$$A \frac{\partial^2 u}{\partial \rho^2} = B \frac{\partial u}{\partial \beta} + C, \quad (A1)$$

where A , B , and C can be functions of ρ , β , and u itself (in the case in hand A and C depend only on ρ , while B depends both on ρ and on u). We make use of a finite-difference scheme, in which the “spacelike” variable ρ and the “time-like” variable β are replaced by the discrete quantities $\rho_j = j\Delta\rho$, $\beta_n = n\Delta\beta$, where $\Delta\rho$ and $\Delta\beta$ are the grid spacings along the ρ and the β directions, and j and n are integers such that $1 \leq j \leq J$, $n \geq 1$. The partial derivatives with respect to ρ and β are then approximated by finite-difference representations [32]. Integration of Eq. (A1) by an *explicit* method (as was done in Ref. [5]), in which the first derivative with respect to β is used directly to update the unknown function u at the temperature step $n+1$ by evaluating all the other terms in the equation at the step n , is in principle straightforward, but it is not recommended for a diffusive equation

like Eq. (20). In fact, as is well known [32], in order to achieve numerical stability those methods require that $\Delta\beta$ must be kept below a certain value $\Delta\beta_{\max} \sim (\Delta\rho)^2/D$, where D is the diffusion coefficient. For Eq. (20) the role of D is played by the expression

$$D = \frac{q}{2} [\rho(1-\rho)]^2 \frac{[1-yF(y)]^2}{(1-y)F'(y) - F(y)[1-F(y)]}$$

$$= \frac{q}{2} [\rho(1-\rho)]^2 \frac{P(z)[1-P(z)] + zP'(z)}{z^2P^2(z)[P(z) - (1-z)P'(z)]},$$
(A2)

where z and $P(z)$ have been defined in Eqs. (7), (8), and y and $F(y)$ are given by $y = [P(z) - 1]/[zP(z)]$, $z = F(y)$. As is readily seen from the expansion (27) for $P(z)$, D diverges whenever the compressibility diverges, namely, at the critical point and on the spinodal curve. To carry out the integration in the critical and subcritical region, one would then be forced to adopt a vanishingly small spacing $\Delta\beta$. It is better then to turn to some *implicit* method, which has the advantage of being unconditionally stable. In such methods the differentiation with respect to β is performed “backward,” so that at a generic temperature step one is left with a set of equations in the J unknowns u_j^{n+1} , $1 \leq j \leq J$. If the original PDE is nonlinear, the resulting equations will in general be nonlinear as well, and the numerical solution can be quite cumbersome. However, for a PDE of *quasilinear* form like Eq. (A1), i.e., such that the “coefficients” A , B , and C do not depend on the partial derivatives of the unknown function u , it is possible to adopt a predictor-corrector algorithm [13] which gives rise only to linear equations. In this procedure every temperature step is split in two and a temporary

value of the unknown function at the step $n + 1/2$ is determined. The scheme is as follows: (1) predictor:

$$A(\rho_j) \frac{u_{j+1}^{n+1/2} - 2u_j^{n+1/2} + u_{j-1}^{n+1/2}}{(\Delta\rho)^2} = B(\rho_j, u_j^n) 2 \frac{u_j^{n+1/2} - u_j^n}{\Delta\beta} + C(\rho_j),$$
(A3)

(2) corrector:

$$\frac{1}{2} A(\rho_j) \left[\frac{u_{j+1}^{n+1} - 2u_j^{n+1} + u_{j-1}^{n+1}}{(\Delta\rho)^2} + \frac{u_{j+1}^n - 2u_j^n + u_{j-1}^n}{(\Delta\rho)^2} \right]$$

$$= B(\rho_j, u_j^{n+1/2}) \frac{u_j^{n+1} - u_j^n}{\Delta\beta} + C(\rho_j).$$
(A4)

The advantage of this method, which rests on the quasilinear structure of the underlying PDE, consists in the fact that one is required to use the updated quantities only in the derivatives and not in the “coefficients,” so that when the predictor and the corrector are solved (respectively, for $u_j^{n+1/2}$ and u_j^{n+1}), one does not get a set of nonlinear equations but rather a linear system of *tridiagonal* type, that can be solved numerically with a small computational effort. For an overall sweep over the whole (ρ, β) plane, we typically adopted a density spacing $\Delta\rho = 10^{-3} - 5 \times 10^{-4}$. When high accuracies were required very close to the critical point, for instance to determine the asymptotic critical regime, values of $\Delta\rho$ about an order of magnitude smaller were used. The inverse temperature spacing $\Delta\beta$ was usually set at $\Delta\beta = 10^{-4}$ at the beginning of the integration, and subsequently decreased to get the critical temperature within a prescribed accuracy. Below the critical temperature, $\Delta\beta$ was then gradually increased up to its initial value. The integration was usually carried down to $T \approx (0.3-0.4)T_c$.

-
- [1] See, for instance, J. P. Hansen and J. R. McDonald, *Theory of Simple Liquids* (Academic, London, 1986).
- [2] J. S. Høye and G. Stell, *J. Chem. Phys.* **67**, 439 (1977). For the special case of the nearest-neighbor lattice gas, the SCOZA was already formulated by Stell, Lebowitz, Baer, and Theumann in the context of the approach they developed in G. Stell *et al.*, *J. Math. Phys.* **7**, 1532 (1966).
- [3] J. S. Høye and G. Stell, *Mol. Phys.* **52**, 1057 (1984); **52**, 1071 (1984).
- [4] J. S. Høye and G. Stell, *Int. J. Thermophys.* **6**, 561 (1985).
- [5] R. Dickman and G. Stell, *Phys. Rev. Lett.* **77**, 996 (1996).
- [6] T. H. Berlin and M. Kac, *Phys. Rev.* **86**, 821 (1952).
- [7] G. Stell, *Phys. Rev.* **184**, 135 (1969).
- [8] A. Parola and L. Reatto, *Nuovo Cimento D* **6**, 215 (1985).
- [9] S. Katsura, T. Morita, S. Inawashiro, T. Horiguchi, and Y. Abe, *J. Math. Phys.* **12**, 892 (1971); **12**, 895 (1971); **12**, 981 (1971); **12**, 986 (1971).
- [10] G. S. Joyce, *J. Math. Phys.* **12**, 1390 (1971).
- [11] G. S. Joyce, *J. Phys. C* **4**, L53 (1971).
- [12] G. S. Joyce, *J. Phys. A* **5**, L65 (1972).
- [13] W. F. Ames, *Numerical Methods for Partial Differential Equations* (Academic, New York, 1977).
- [14] C. F. Baillie *et al.*, *Phys. Rev. B* **45**, 10 438 (1992).
- [15] A. J. Liu and M. E. Fisher, *Physica A* **156**, 35 (1989).
- [16] See, for instance, D. M. Burley, in *Phase Transitions and Critical Phenomena*, edited by C. Domb and M. S. Green (Academic Press, London, 1972), Vol. 2.
- [17] R. J. Baxter and P. J. Forrester, *J. Phys. A* **17**, 2675 (1984).
- [18] D. Pini, A. Parola, and L. Reatto, *J. Stat. Phys.* **72**, 1179 (1993).
- [19] M. F. Sykes, D. S. Gaunt, P. D. Roberts, and J. A. Wyles, *J. Phys. A* **5**, 640 (1972).
- [20] M. E. Fisher and R. J. Burford, *Phys. Rev.* **156**, 583 (1967).
- [21] H. B. Tarko and M. E. Fisher, *Phys. Rev. B* **11**, 1217 (1975).
- [22] M. F. Sykes, D. L. Hunter, D. S. McKenzie, and B. R. Heap, *J. Phys. A* **5**, 667 (1972).
- [23] J. W. Essam and M. E. Fisher, *J. Chem. Phys.* **38**, 802 (1963).
- [24] R. Kikuchi, *Phys. Rev.* **81**, 988 (1951).
- [25] See, for instance, A. M. Ferrenberg and D. P. Landau, *Phys. Rev. B* **44**, 5081 (1991); and Ref. [15].
- [26] A. Parola and L. Reatto, *Phys. Rev. A* **31**, 3309 (1985).
- [27] A. Parola and L. Reatto, *Adv. Phys.* **44**, 211 (1995).
- [28] J. S. Høye, D. Pini, and G. Stell (unpublished).

- [29] G. Stell, Phys. Rev. **173**, 314 (1968).
- [30] M. E. Fisher and B. U. Felderhof, Ann. Phys. (N.Y.) **58**, 217 (1970).
- [31] D. Pini, G. Stell, and J. S. Høye, SUSB College of Engineering and Applied Sciences Report No. 738, 1997 (unpublished).
- [32] W. H. Press, B. P. Flannery, S. A. Teukolsky, and W. T. Vetterling, *Numerical Recipes* (Cambridge University Press, Cambridge, England, 1992), Sec. 19.2.